Brownian dynamics simulations of aging colloidal gels

Rodolphe J. M. d'Arjuzon*
Cavendish Laboratory, University of Cambridge, Madingley Road, Cambridge CB3 0HE, United Kingdom

William Frith and John R. Melrose
Colworth House, Unilever Research, Bedford, United Kingdom

(Received 14 October 2002; published 25 June 2003)

The aging of colloidal gels is investigated using very long duration Brownian dynamics simulations. The Asakura-Oosawa description of the depletion interaction is used to model a simple colloid polymer mixture. Several regimes are identified during gel formation. The intermediate scattering function displays a double decay characteristic of systems where some kinetic processes are frozen. The β relaxation at short times is explained in terms of the Krall-Weitz model for the decorrelation due to the elastic modes present. The α relaxation at long times is well described by a stretched exponential, showing a wide spectrum of relaxation times for which the q dependence is $\tau_\alpha = q^{-2.2}$, lower than for diffusion. For the shortest waiting times, a combination of two stretched exponentials is used, suggesting a bimodal distribution. The extracted relaxation times vary with waiting time as $\tau_\alpha = \tau_w^{0.66}$, more slowly than in the simple aging case. The real space displacements are found to be strongly non-Gaussian, correlated in space and time. We were unable to find clear evidence that the gel aging was driven by internal stresses. Rather, we hypothesize that in this case of weakly interacting gels, the aging behavior arises due to the thermal diffusion of strands, constrained by the percolating network, which ruptures discontinuously. Although the mechanisms differ, the similarity of some of the results to aging of glasses is striking.

DOI: 10.1103/PhysRevE.67.061404 PACS number(s): 82.70.Dd, 61.43.Hv, 61.20.Lc

I. INTRODUCTION

Like other nonequilibrium phenomena, colloidal gelation has attracted considerable interest in the last 20 years. Colloids are found in many forms and are highly relevant for industry. Muds, paints, cosmetics, and many food products are examples where understanding of colloid science is essential in the design of product properties. Studies can be conducted over a wide range of densities, and the interactions can be finely tuned in terms of range and depth of potential by altering the particle coating, solvent conditions, or solutes present.

Importantly, under certain conditions it is possible to make colloid particles form a macroscopic gel. Although there is no universal definition, a gel is usually understood to be a percolating viscoelastic network that has no long range order (although it may have some local order), but a characteristic length scale is present; gels are usually fractals at low volume fractions but this is not a necessity. Common examples of colloid gels include yogurt, toothpaste, and clays.

The system under study here is a colloid polymer mixture. Such systems have been known to have interesting equilibrium and nonequilibrium properties for many years [1]; they are also a stepping stone to understanding the more complicated mixtures that make up many ordinary products: shampoo and paint are examples that involve complex polymer colloid mixtures. Such systems can display depletion flocculation, and the resulting gels are often used as one of the simplest models of weakly attractive systems due to their relative simplicity arising from the absence of charge effects.

The properties of nonequilibrium systems as they age are not only relevant for applications, but are also a crucial step to understanding the very nature of gels. Indeed, if slow aging were not a feature of the gels, phase separations would only result in equilibrium phases.

The dramatic slowdown of the dynamics in gels has prompted investigations into their possible link with glasses. While gels are usually found at lower volume fractions and when strong interparticle interactions are present, colloid glasses are usually found at high volume fractions, above $\phi = 0.58$, or for deep quenches. They share many properties such as being out of equilibrium, nonergodic, lacking long range order, and having slow dynamics. Since work on the glasses and their aging is extremely topical in soft condensed matter, this work will look for similarities between the aging of colloid gels and glasses.

There is abundant literature on gels and on colloid polymer systems in particular. Asakura and Oosawa were the first to describe the attraction between colloid particles when nonadsorbing polymer is present in solution [2]. The depletion mechanism that is responsible for this can be understood in different ways. The essential point is the presence of a region around the colloids from where the polymer coil center of mass is excluded. When two colloid particles come together the regions of excluded volume overlap, resulting in an increase of the free volume available to the polymer, causing an increase of their entropy and an overall decrease of the free energy of the system. The problem can also be analyzed in terms of the net osmotic pressure on a pair of colloids as they come together.

Theoretical work on the system was done by Vrij [3], who independently rediscovered the Asakura and Oosawa model, and demonstrated the presence of spinodal instability in the

*Electronic address: rjmd2@phy.cam.ac.uk

system. Gast *et al.* treated the polymer as a perturbation to the hard sphere results, thus producing the first phase diagrams [4,5]. Lekkerkerker *et al.* [6] used a free volume approach to treat this problem while Djikstra *et al.* formally integrated out polymer degrees of freedom [7]. It has been shown that for size ratios below $k=0.154$ there can be no three-body interactions and that the two-body Asakura-Oosawa (AO) potential can therefore be an adequate description. A review of the details of the different approaches to the colloid polymer system can be found in [7]. It is important to note that the depletion potential gives well controlled systems where the interparticle interaction potential well is usually in the range of $(1-10)kT$, very different from emulsions, for example, where the interaction energy can be of order $100kT$.

Felicity *et al.* [8] and Lodge and Heyes [9] modeled colloid gels interacting via a Lennard-Jones potential and studied their viscoelastic properties [9,10]; Bijsterbosch *et al.* investigated fractal colloidal gels for various interactions using Brownian dynamics simulation methods [11]. Dickinson [12], and Bos and van Opheusden [13] have worked on stress relaxations after shear stresses were applied. Soga *et al.* have worked on percolation [14] and phase transitions [15] in the colloid polymer system. The yielding behavior of two-dimensional (2D) colloid gels was investigated by West *et al.* [16].

Experimentally, most notable was the work of Grant and Russel [17], Poon *et al.* [1], Lekkerkerker *et al.* [18], and Verduin and Dhont [19]. An important result from all of these works was that at moderate volume fractions ($0.1<\phi<0.4$) gelation can be expected to occur for high polymer concentrations (deep quenches). Also, for ranges of interaction of less than one-third of the particle diameter, no liquid phase formed; the liquid-gas binodal becoming metastable with respect to fluid-solid phase separation. In light scattering, the gelation is marked by the ''freezing'' of the evolution of the low q peaks, demonstrating that the dynamics become arrested as the sol-gel transition is reached.

The following experiments are explained in more detail since they contain the most interesting data for comparison with our simulations. Cipelletti *et al.* [20] have produced experimental results on the aging of polystyrene colloid gels at low volume fractions ($10^{-4}<\phi<10^{-3}$). The gels were formed by aggregation due to the van der Waals forces, and were found to be fractal. The aging behavior was sampled for waiting time going from hours to ten days, the relaxations were stretched exponentials with the exponent greater than 1. The unusual scattering vector dependence of the relaxation times, $\tau_f \propto q^{-1}$, was explained in terms of a dipole elastic field caused by the high internal stresses of the gels. The waiting time dependence of the relaxation times was nearly linear, $\tau \propto \tau_w^{0.9}$, following a period of exponential growth (this exponential regime was also observed in an aging clay suspension [21]).

The same group, in a series of rheology and dynamic light scattering experiments, also found the same behavior in a system composed of multilamellar vesicles, where, once again, it was thought to be the strong internal *repulsive* stresses that dominate the response [22].

Experiments on the dynamics of colloidal gels have been performed by Krall and Weitz [23] for the short time (or β, see below) relaxations. They also presented a model for the elastic modes present in a fractal gel, from which the mean squared displacements of strands constrained by the network can be calculated. Working on gels at densities comparable with this work, Romer *et al.* [24], showed that the predictions of this model held even for nonfractal structures.

Both short and long time scale dynamics were observed by Solomon and Varadan [25] in their study of adhesive colloids at low volume fractions and for interparticle interaction strengths close to that used in this work ($10kT$). The Krall-Weitz model was used at short times, with a simple exponential observed at long times.

A commonly calculated quantity is the intermediate scattering function (ISF), a time dependent correlation function. When looking at glasses and gels the self-part of the ISF will display a double decay: at short times a fast decay often referred to as the β relaxation, and at long times a second decay called the α relaxation. Structural arrest, brought about by increased density for hard spheres or by quenching for a Lennard-Jones system, leads to a wide separation of these time scales and the appearance of a plateau at intermediate times (see Ref. [26] and references therein). Since the scattering function is wave vector dependent, spatial information can also be obtained.

The α and β relaxations are often explained in terms of the cage effect. For a system of purely repulsive particles, a particle is confined by its neighbors which form a cage around it; the particle is free to diffuse within its cage, thus setting the β time scale. The time required for the particle to diffuse out of the cage is the α time scale. As a system becomes denser, cage rearrangements become increasingly difficult, causing the α relaxations to occur on longer time scales. For systems of attractive particles, one can talk about an open cage, whereby a particle would be confined to its neighbors because of the attractive forces. This also results in two relaxation time scales. On this basis it has been argued that the gel transition should be described in terms of mode coupling theory (MCT) as an ergodicity breaking transition [27–30]. MCT has helped considerably in understanding supercooled liquids [26] and high volume fraction colloid glasses [31], and its predictions are now being tested for gels as well [25]. The kinetic arrest of gels has also been reported by Segré *et al.* [32], who compared it to the features of the hard sphere colloid glass transition.

Ideal MCT assumes closeness to equilibrium and is therefore useful only for the fluid-gel transition. Nonequilibrium MCT has also been developed by Bouchaud *et al.* [33]; this predicts aging behavior. Some of these predictions have been qualitatively tested on a Laponite glass [21]. However, earlier theoretical models have been shown to have interesting aging properties. For example, Cugliandolo and Kurchan solved the spin glass model for out of equilibrium dynamics [34]. Crucially, these equations are identical to those produced by some MCT models.

Another approach to explaining the behavior of glasses has been the study of the properties of the potential energy surface (PES) as proposed by Goldstein [35]. One model that

uses this concept is the successful trap model of Bouchaud [36] which has been widely applied for spin glasses and of which many variants exist. This was one of the first models to make useful predictions about aging. Another formalism is now introduced to facilitate discussion. The inherent structures (IS's) of a system are defined as the local minima of the PES; all points in configuration space which end up in the same IS following a steepest decent path define the basin of that IS [37]. Sciortino and Tartaglia distinguish between four dynamical regimes. There is a high temperature region where the system is fluid; an intermediate region where the system is always close to the ridges separating the different basins, this being the regime in which MCT is successful; and a third regime is found at low T where the system populates IS's with lower and lower energy. When the time of escape from a basin becomes longer than the experimental time scale the system no longer equilibrates; this is the fourth regime, normally called a glass [38]. In this formalism the two-step relaxation of the correlation function is seen as decoupling of the fast (intrawell) vibrational excitations and the slower rearrangements corresponding to the system sampling different basins, which for low T may require activated processes.

It is useful to set up a few hypotheses about the possible causes of aging in gels. First, very slow crystallization about some locally highly ordered regions is a possibility, although this is not normally seen in experiments. Second, the aging may be stress driven, as was argued in order to explain the results of experiments on some experimental systems [20,22]. Third, thermal fluctuations and random breaking of bonds may allow relaxation of the network as suggested by Solomon and Varadan [25]. Compactification of strands up to a point where they might dislocate has also been suggested as a possibility to explain the collapse of transient gels [39].

II. METHODS

A. The model

The Brownian dynamics model is based on a Langevin type equation of motion for each colloid particle with a fluctuating random force accounting for the thermal collisions of the solvent molecules with the particle. The polymer coils are not simulated, their presence being felt only through the attractive potential between the colloids:

$$M\ddot{\boldsymbol{X}} = \boldsymbol{F}^C + \boldsymbol{F}^B + \boldsymbol{F}^D = \boldsymbol{0}, \tag{1}$$

where M and $\boldsymbol{X}$ are the inertia and position matrices, respectively; $\boldsymbol{F}^C$ are the conservative forces, $\boldsymbol{F}^B$ are the random Brownian forces, and $\boldsymbol{F}^D$ are the dissipative drag forces. This last term encompasses all the hydrodynamic interactions, which couple the forces on the particles through the solvent. It is these forces that oppose the relative motion of the particles and are most important in flow. They will affect nonequilibrium phenomena at rest, but in common with many others we neglect the many body interactions in this study. In this model, this term is reduced to the Stokes drag for a spherical particle (α), applied individually: this is the free draining approximation. So the drag force on each particle satisfies the relation

$$\boldsymbol{f}_i^D = -\alpha \boldsymbol{v}_i = -6\pi\eta d\boldsymbol{v}_i, \tag{2}$$

where η is the viscosity of the liquid, d is the particle diameter, and $\boldsymbol{v}_i$ is the velocity of particle i.

The inertia terms are neglected so this becomes a force balance equation, which is solved for the displacements of the particles. The conservative forces are the sum of a steep core potential and the depletion force obtained via the following two-body potential energy term:

$$U = \frac{1}{2}\sum_{ij}\left[U_{HC}(r_{ij}) + U_{AO}(r_{ij})\right], \tag{3}$$

where the first term U_{HC} is the power law repulsive hard core,

$$\frac{U_{HC}}{kT} = \left(\frac{r_{ij}}{d}\right)^{-n}. \tag{4}$$

$n=36$ is used to avoid anomalies that may result from having a softer potential [40] while retaining computer time efficiency. The two-body depletion potential used was

$$\frac{U_{AO}}{kT} = QH(L,r_{ij})\left[L^2\frac{r_{ij}}{d} - \frac{1}{3}\left(\frac{r_{ij}}{d}\right)^3 - A\right], \tag{5}$$

where r_{ij} is the separation between spheres i and j, and d is the diameter of the colloid particles. If k is the size (diameter) ratio between a polymer and a particle at the polymer volume fraction ϕ_p, then

$$L = 1 + k,$$

$$A = \frac{2L^3}{3},$$

$$Q = \frac{3\phi_p}{2k^3},$$

$$H\left(L, \frac{r_{ij}}{d}\right) = \begin{cases} 1, & \dfrac{r_{ij}}{d} < L \\ 0, & \dfrac{r_{ij}}{d} > L. \end{cases} \tag{6}$$

Strictly speaking, the parameter $\phi_p = \frac{1}{6}\pi k^3 d^3 n_R$, where n_R is the polymer number density in a reservoir of pure polymer which would match the chemical potential of the polymer solution with colloid particles at volume fraction ϕ [6]. It is useful that the potential used here is of finite range, as this avoids truncation errors and allows us to define the nearest neighbors and interacting particles precisely.

The Brownian forces represent the action of the liquid molecules averaged out over one time step. They average out to zero, and are uncorrelated in time:

$$\langle \boldsymbol{F}_B \rangle = 0, \tag{7}$$

$$\langle \boldsymbol{F}_B(t)\boldsymbol{F}_B(t') \rangle = 2\pi\alpha k_B T \delta(t-t'). \tag{8}$$

The fluctuation-dissipation theorem relates the magnitudes of $\boldsymbol{F}_B$ and α by enforcing that every squared separable degree of freedom satisfies the equipartition theorem.

In order to simplify the calculation, reduced units are used in the simulation, k_BT becoming the energy unit. The polymer volume fraction ϕ_p is the only control parameter for the depth of the potential, and the ratio of the colloid to polymer size k controls the range of the potential. This was fixed at $k=0.1$ for all simulations shown here.

All distances are measured in units of the colloid particle's diameter d.

The natural time unit to use is the Brownian relaxation time. It is defined as the time for a particle to diffuse its own length scale by Brownian motion,

$$\tau_R = \frac{\eta d^3}{k_B T}. \tag{9}$$

For a micrometer size particle in water, τ_R is of the order of 0.2 s. Note, however, the strong dependence on particle size. The typical length of runs shown here was $5000\tau_R$ and the longest run was twice that. This is a great increase compared to previous studies, which were typically run for about $100\tau_R$.

The system being simulated is a three-dimensional cubic box with 4000 particles in periodic boundary conditions.

B. Quantities of interest

As mentioned earlier, the self-part of the intermediate scattering function (also called the incoherent intermediate scattering function) gives information about the relaxation of density fluctuations in the sample. It lets us assess whether particles are displaced on a length scale set by $2\pi/\boldsymbol{q}$ or whether kinetic processes of that wavelength are ''frozen out.'' It is a commonly calculated quantity as it can be measured in light scattering experiments [20]. It is calculated from simulation data by

$$F_s(q,t,t_w) = \frac{1}{N}\sum_i e^{i\boldsymbol{q}\cdot[\boldsymbol{r}_i(t_w)-\boldsymbol{r}_i(t_w+t)]}, \tag{10}$$

where t_w is the waiting time for that sample. In periodic boundary conditions we can consider only a closed set of wave vectors $\boldsymbol{q}$. Therefore, for each axis we have

$$q = \frac{2\pi n}{L}, \quad n = 0,1,2,\ldots,$$

with L the linear dimension of the box. To improve the statistics the results are averaged over the x, y, and z axes. Since it depends on both t and t_w, F_S is a so-called *two-time quantity*, which is most useful in determining and characterizing any aging behavior if it is present.

In order to calculate particle correlations in real space the radial distribution function $g(r)$ is calculated, as well as the self-part of the Van Hove correlation function, which samples particle displacements in time:

$$g(r) = \frac{1}{\langle n \rangle}\sum_{i\neq j}^{N} \delta(|\boldsymbol{r}_i - \boldsymbol{r}_j| - \boldsymbol{r}),$$

where $\langle n \rangle$ is the average number density, and

$$G_s(r,t) = \frac{1}{N}\sum_i^N \langle \delta(|r_i(t) - r_i(0)| - r) \rangle,$$

where $\langle \cdots \rangle$ is an average over time origins. The quantity

$$S(r,t) = 4\pi r^2 G_s(r,t)$$

gives the probability of finding a particle at a distance r after a time t, and $G_s(r,0) = g(r)$.

In the Gaussian approximation,

$$G_s(r,t) = \frac{1}{(4\pi D t)^{3/2}} \exp\left(\frac{-r^2}{4Dt}\right),$$

which is a solution of the diffusion equation.

Our results are divided into two parts; the first part will be concerned with ''macroscopic'' quantities, i.e., correlation functions and quantities that have been averaged over several systems; the second part will look more closely at the ''microscopics'' of individual systems.

III. RESULTS

A. Macroscopics

As in previous simulations [14,15] the samples were equilibrated at high temperature ($\phi = 0$) and instantaneously quenched to an appropriate value of ϕ_p. Work in [15] determined that for $\phi_p \geqslant 0.3$ crystals were no longer obtained. For these relatively deep quenches, amorphous, nonequilibrium structures were obtained; these networks come under the general name of gels or transient gels when seen experimentally before they collapse under gravity. They are qualitatively similar to gels created experimentally and Lennard-Jones (LJ) gels from simulations. All gels considered here have $\phi = 0.30$ and $\phi_p = 0.40$, giving a potential minimum of $U_{min} = -8kT$. Properties are averaged over five samples unless otherwise stated.

In Fig. 1 the potential energy of the system U is scaled by $U \rightarrow 2U/NU_{min}$, giving the approximate number of neighbors assuming interparticle distances are near the potential minimum. The gel particles have approximately seven neighbors. It is immediately obvious that we are dealing with a nonequilibrium system since, after the initial very fast drop in energy after quenching, a long regime of slow decay is entered; no equilibrium value was ever reached in the simulations we ran. Such small decays can be fitted with a number of functions; however, for comparison with Kob and Barrat [41], it was fitted with a power law $U = at^{-b}$, as shown in the inset of Fig. 1, yielding $b = 0.3$.

It is revealing to look at the total number of bonds in the system as gelation occurs. When plotted on log-linear scale

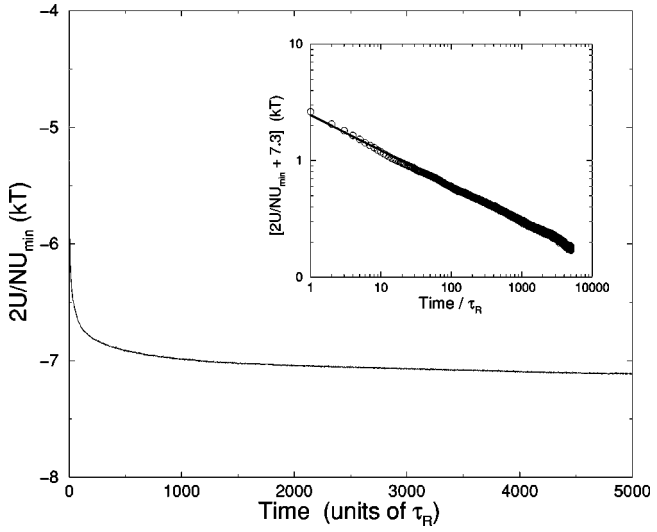

FIG. 1. Potential energy of gel, from formation to aging. The fit for the inset is a power law.

(Fig. 2) three different growth regimes are evident, the first up to $10\tau_R$, another from $10\tau_R$ to around $100\tau_R$, and the last one from there on. Note that, since the ordinate range is small, a log-log plot shows practically the same result; hence one cannot easily distinguish between a low power law growth and logarithmic growth. The fits are of the form $N = c\log(t)+d$, where the values of c are shown on the plot. As explained in the discussion we are here mostly concerned with behavior over the last of these regimes.

The ISF was found to display the expected two-step relaxation at short (β relaxation) and long (α relaxation) times. These time scales are treated separately here since the averaging cannot be done in the same way. For the waiting time independent β relaxation an average over time origins can be used, whereas for the α relaxation the nonergodic nature of the system means that only an ensemble average can be performed.

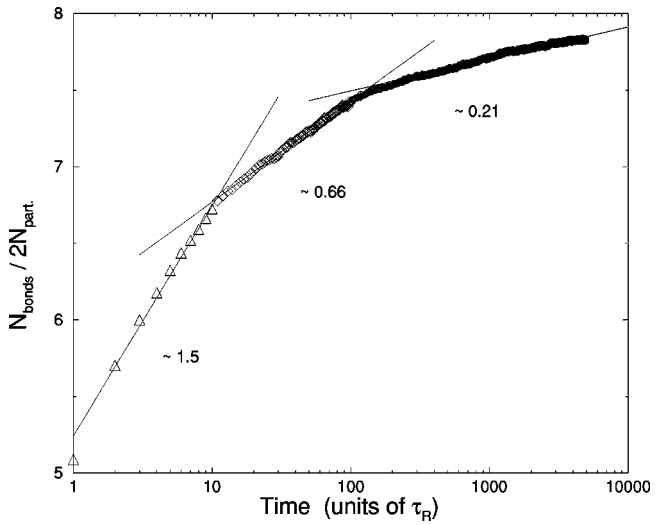

FIG. 2. Total number of bonds in the gel. The three straight lines and their gradient are superposed to highlight the three different logarithmic regimes.

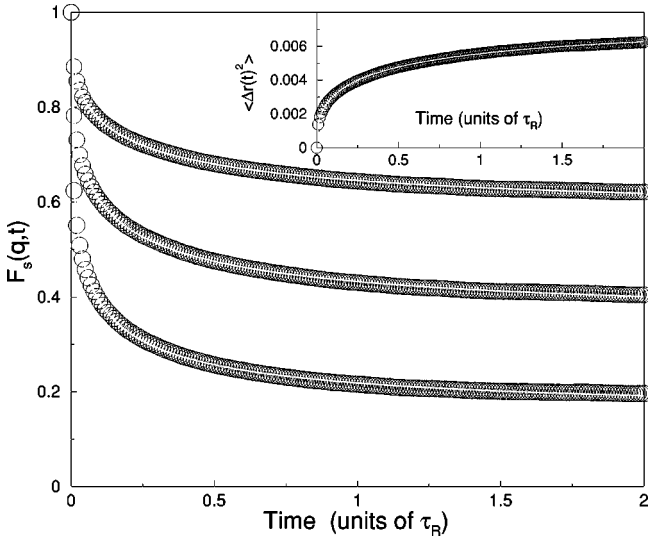

FIG. 3. β relaxation at short times for $qd=23.0$, 32.9, 46.0, with stretched exponential fits given in text (white line). Inset: mean squared displacement (black circles) for the same time scale with fit to Eq. (11) (white line).

Figure 3 shows the initial β relaxation decay for increasing values of q. As the gel forms, the mean squared displacements of the particles are Fickian, but as aggregation proceeds the behavior becomes subdiffusive [$\langle\Delta r(\tau)^2\rangle \propto t^e$, $e<1$]. Finally, for measurements in the region of interest the mean squared displacement takes on the form of Fig. 3 (inset), where a plateau is reached at displacements that are small compared to the particle size. This is interpreted in terms of the Krall-Weitz model for the initial decay of the correlation function [23]. This model considers the relaxation due to the elastic modes present in the gel, with the particles assumed to be confined to the gel strands. Their conclusion was that the mean squared displacement should obey

$$\langle\Delta r(\tau)^2\rangle = \delta^2[1-e^{(-\tau/\tau_\beta)^p}]. \tag{11}$$

The particle displacements are constrained to an amplitude δ; the stretched exponential form comes about from the sum of the relaxations on all length scales.

Consistently with the model we are using, the β decay was fitted with the following law which is closely related to a stretched exponential:

$$F_s(\boldsymbol{q},t) = \exp[\boldsymbol{q}^2\langle\Delta r^2(t)\rangle/6] \tag{12}$$

for all $\boldsymbol{q}$ vectors, with $\langle\Delta r^2(t)\rangle$ from Eq. (11). The results are shown in Fig. 3 for three different values of $\boldsymbol{q}$. The values of the parameters were determined by fitting Eqs. (11) and (12) to the data in Fig. 3. The fit parameters were $p=0.4\pm0.1$, $\delta=(0.075\pm0.004)d$, and $\tau_\beta=(0.26\pm0.04)\tau_R$.

The maximum mean squared displacement δ^2 (excluding any α processes) sets the height of the plateau in F_s via $F_s(q,t)=(1/N)\Sigma_i e^{-q^2(\Delta r_i^2)/6}=f_q^s$, where f_q^s is the nonergodicity parameter for the incoherent scattering. Figure 4 shows that the nonergodicity parameter decays exponentially for increasing q; δ^2 can then be extracted since $f_q=e^{-(q\delta)^2/6}$ in

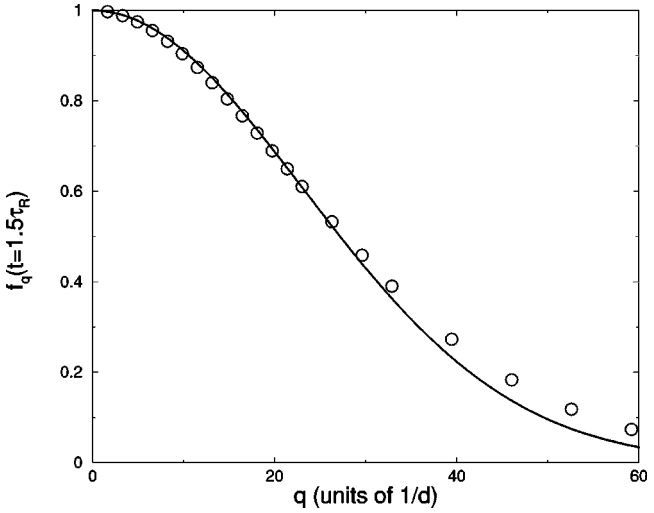

FIG. 4. Nonergodicity parameter as a function of q, with exponential fit.

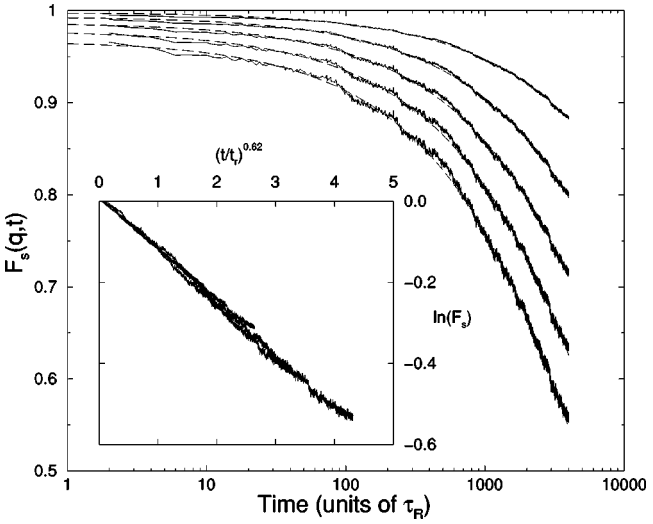

FIG. 5. q vector dependence of the intermediate scattering function for long times and fits to Eq. (12). From top curve $qd=2.30$, 3.28, 4.27, 5.26, 6.25. The waiting time is $1000\tau_R$. Inset: collapse of the same data when scaled as described in text and plotted against stretched time.

the Gaussian approximation. The previously extracted value of δ was used for the fit. However, there is a small ambiguity about where exactly f_q should be measured, since when α processes are also present there is no true plateau; in this case the values of f_q were measured after $1.5\tau_R$.

We now turn to the long time dynamics. The second decay (α relaxation) is the part of the dynamics that is expected to show signs of aging. Because the system is nonergodic, an ensemble average cannot be replaced by a time average. Unfortunately, very long runs are needed in order to get to the time scales that are relevant for this study, and therefore only a limited number of runs can be performed due to computer time limitations. The averages were therefore performed over a set of five runs. Information about the dynamics on different wavelengths can be extracted by looking at data from a fixed waiting time and sampling at different q. For a given q the waiting times were then varied to observe the aging in the dynamics.

Figure 5 shows the α relaxations for a single waiting time and the q vectors $qd=2.3$, 3.28, 4.27, 5.26, and 6.25. The relaxations were fitted to a stretched exponential law:

$$F_s(q,t)=A\exp\{-[(t-t_w)/\tau_\alpha(q)]^\mu\}, \tag{13}$$

where A is a constant chosen to be the plateau height and μ is kept constant for different q. The data collapse onto a master curve when plotted as a function of stretched time $(t-t_w)^\mu$ once normalized by A and τ_q (inset of Fig. 5). The relaxation times $\tau_\alpha(q)$, which are extracted from the fits for different q, were found to follow a power law relationship

$$\tau_\alpha \sim q^{-\nu}$$

with $\nu=\nu(t_w)$. The best fit values extracted were slightly age dependent, as summarized in Table I.

For waiting times $t_w \leqslant 1000\tau_R$, values of μ decreased, and it was noticed that the quality of the fits decreased, becoming impossible for $t_w < 500\tau_R$. The α relaxation at these early times displayed a relatively fast decay followed by a slower one (see the curves for $t_w=20\tau_{\hat{R}}$ and $100\tau_R$ in Fig. 6). These relaxations were fitted with a double stretched exponential:

$$F_s(q,t)=\frac{f_q}{(1+A_1)}\left\{\exp\left[-\left(\frac{t-t_w}{\tau'_{\alpha1}}\right)^{\mu'_1}\right] + A_1\exp\left[-\left(\frac{t-t_w}{\tau'_{\alpha2}}\right)^{\mu'_2}\right]\right\}. \tag{14}$$

The justification for this law is given in the discussion section. Once again the relaxation times contain wavelength dependent information, $\tau'_{\alpha2}\sim q^{\nu'_2}$; from the fits $\nu'_2\approx 2.2$ for all appropriate waiting times as summarized in Table I. $\tau'_{\alpha2}$ was found to depend only very weakly on q. The exponent $\mu'_2=0.7$ was held constant and f_q was used to give the correct plateau height.

The significance of these exponents is discussed in the next section.

TABLE I. Summary of the exponents as a function of age of the gel.

t_w/τ_R	μ	ν	Double exponential	μ'_1	μ'_2	ν'_2
100			Y	0.7	0.7	2.2
200			Y	0.85	0.7	2.1
500	0.45	3.0	Y/N	0.9	0.7	2.2
750	0.50	2.7	N			
1000	0.62	2.5	N			
1250	0.70	2.3	N			
1500	0.70	2.3	N			
2000	0.72	2.2	N			

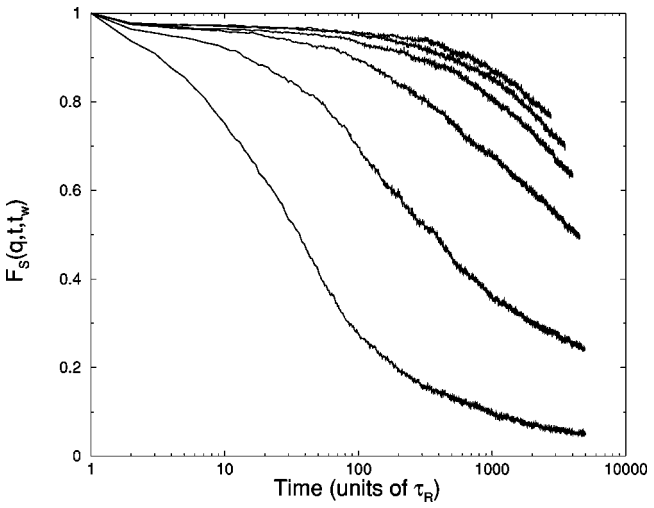

FIG. 6. Intermediate scattering function at fixed $qd=6.25$ and increasing waiting times, from left, $t_w=20\tau_R$, $100\tau_R$, $500\tau_R$, $1500\tau_R$, $2250\tau_R$.

Figure 6 shows the aging behavior of the gels. The data were all collected at a single q value, $qd=6.25$. The smallest waiting time considered here is $20\tau_R$. As the waiting times were increased from $20\tau_R$ up to $2250\tau_R$ a lengthening of the β plateau was observed, with the relaxation of the system becoming slower with increasing waiting time. This is classic aging behavior for nonequilibrium systems and glasses and has been seen for supercooled LJ systems by Kob and Barrat [41].

The data collapse of the α decay is often observed in experiments on glasses, where one finds that each set of data can be scaled using a single time scale which encompasses the whole parameter dependence [42]. Hence the following scaling:

$$F_s(q,t,t_w)\sim\tilde{F}(t/\tau_\gamma)$$

with $\tau_\gamma=\tau_\gamma(t_w)$. Using an arbitrary value of $F_s=0.71$ to define a relaxation time for each curve $\tau_\gamma=t(F_s=0.71)$, the results were rescaled and replotted on Fig. 7 using waiting times $\geqslant 100\tau_R$. The lower limit was chosen to be at the start of the last regime seen in Fig. 2. As can be seen, the data in the range considered appear to collapse well. This relatively good collapse is surprising in that the exponent of the stretched exponential μ varies with waiting time.

Figure 8 shows the dependence of τ_γ on t_w. The interpretation of the results in Fig. 8 is slightly ambiguous. It is possible to interpret these data in two ways: first, in terms of a single power law regime $\tau_\gamma\sim t_w^\xi$ with $\xi=1.26$; second, in terms of two power law regimes, the first with $\xi=1.33$ and the second with $\xi=0.62$, the separation between the regimes being around $t_w=1000\tau_R$. All of these possible values for ξ are not far from 1, which is similar to the aforementioned results of Kob and Barrat [41]. It was also checked that the same behavior resulted if values of τ_α were extracted directly from the fitted stretched exponentials. The issue of one or two regimes will be discussed further on.

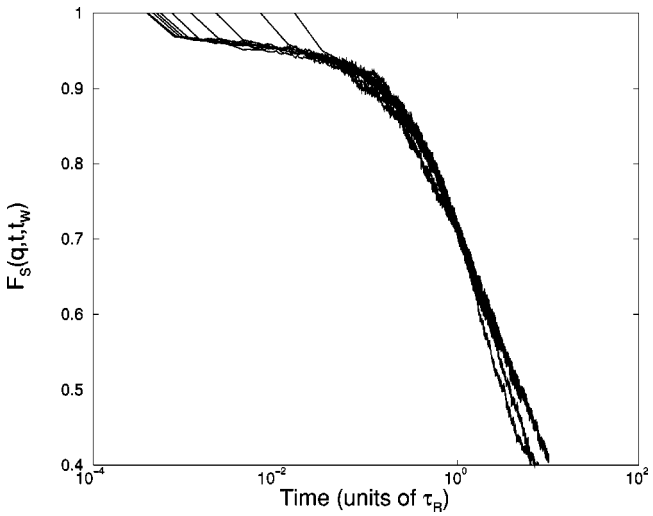

FIG. 7. Intermediate scattering curves made to coincide at $F_s=0.71$.

Another scaling was proposed by Müssel and Rieger for the LJ supercooled fluid results [43] and was attempted for comparison. $F_s(q,t,t_w)\sim\tilde{F}\{\ln[(t+t_w)/\mu]/\ln(t_w/\mu)\}$, where μ is a fit parameter and plays the role of an effective microscopic length scale. This was proposed by Fisher and Huse in the context of spin glasses [44]. This scaling was also applied to our data; however, it did not produce a successful collapse.

B. Microscopics

Over the period of time considered, it is seen that, although the average number of bonds in the system increases, there is little increased crystallinity as shown by the local order parameter, denoted ψ_x (main part of Fig. 9). The local crystalline order parameter is defined as the fraction of particles that are 12 coordinated or neighboring a 12 coordinated site. The inset of Fig. 9 shows the probability density distribution of the coordination of the particles in the system. The initial crystallinity, which is present very soon after the

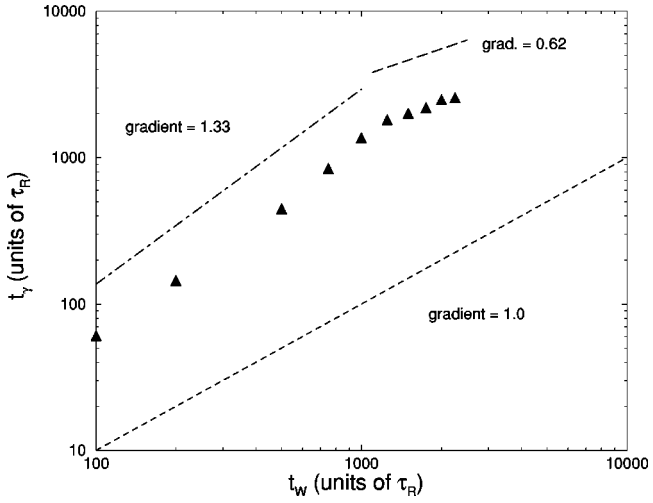

FIG. 8. Relaxation times extracted from the rescaling of Fig. 6.

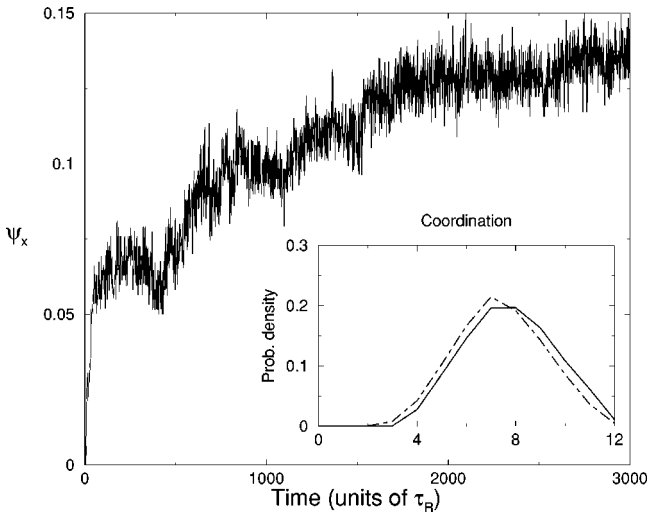

FIG. 9. Crystalline order parameter. Inset: distribution of particle coordinations in gel: solid line, $t_w = 3000\tau_R$; dot-dashed line, $t_w = 100\tau_R$.

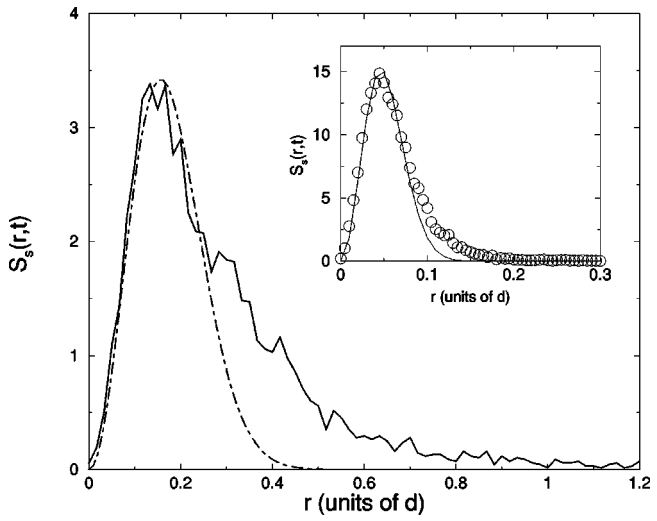

FIG. 10. Self-part of the Van Hove correlation function. Main graph: long time interval, $\delta t = 3000\tau_R$. Inset: short time interval, $\delta t = 10\tau_R$. The peak area is fitted with a Gaussian, shown as a dot-dashed line.

quench, is just the result of the high initial colloid volume fraction together with the strong local order, which is itself due to the lack of angular rigidity of the bonds. There is therefore no ambiguity about a gel with a nonzero crystalline local order parameter. At later times an increase of the average position of the peak is seen, but no significant increase in crystallinity. This already rules out one of the possible hypotheses for the aging of the gel, namely, slow growth of crystals around the crystallites present from formation.

In order to obtain a better understanding of the relaxation mechanisms at work, the particle dynamics are sampled in real space through the Van Hove correlation function. $S(r,t)$ gives the probability of finding a particle at time $t+\delta t$ at a distance r from its position at time t. Due to the nonergodicity, it is not possible to time average this correlation function either. However, the accuracy of this result was checked by averaging over a time interval that was short compared with the typical α relaxation time scale. Figure 10 shows a pair of typical results; they were calculated for $t_w = 3000\tau_R$ and $\delta t = 50\tau_R$ and $3000\tau_R$ for the short and long time intervals, respectively. For these parameters we expect to be in the β plateau for the former time interval and in the α relaxation regime for the latter. Indeed, the peaks of the distributions are around $0.05d$ and $0.16d$, which are consistent with earlier deductions about those regimes. Also shown on Fig. 10 are the Gaussian fits for the peaks and the regions around them. The difference in the behavior of the dynamics in those two regimes can here be seen more intuitively. For times up to and including the β plateau, the gel particles' displacements are nearly Gaussian, consistent with a diffusionlike mechanism. The main part of the plot shows the displacements during the α relaxation regime; the distribution is very much broader, with the longer displacements not fitting within a Gaussian. The displacements found after the peak follow a power law $S(r,t) \sim r^{-f}$, with $f = 2.8 \pm 0.4$.

The strongly non-Gaussian displacements rule out a diffusive mechanism and hint at cooperative motion. This can be seen visually when color coding particle displacements on a three-dimensional (3D) representation of the gel (not shown here). Clusters of particles are observed to be displaced by similar amounts; in fact, this was also true when color coding displacements that were less than the peak value. In order to show the presence of collective displacements clearly, a velocity correlation function was calculated:

$$C_v(r) = \frac{1}{NW} \sum_{ij}^{N} \langle \delta(r-(r_i-r_j)) \boldsymbol{v}(r_i) \cdot \boldsymbol{v}(r_j) \rangle, \quad (15)$$

where $W = \Sigma_i^N \langle \boldsymbol{v}(r_i) \cdot \boldsymbol{v}(r_i) \rangle$ is used to normalize C_v. This is shown in Fig. 11 for $t_w = 4000\tau_R$ and velocities calculated over an interval of $\Delta t = 50\tau_R$. The data are fitted with an exponential, allowing a characteristic correlation length $r_v = 1.9d$ to be extracted. An interesting point was that the results for the velocity correlation function, for all times be-

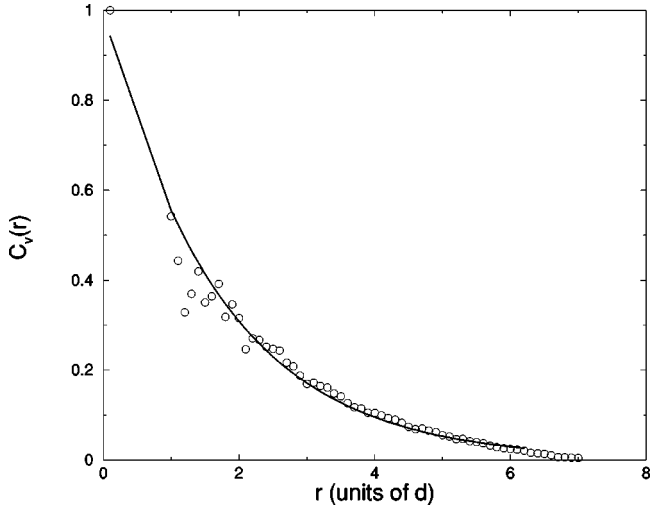

FIG. 11. Displacement correlation function, with an exponential fit.

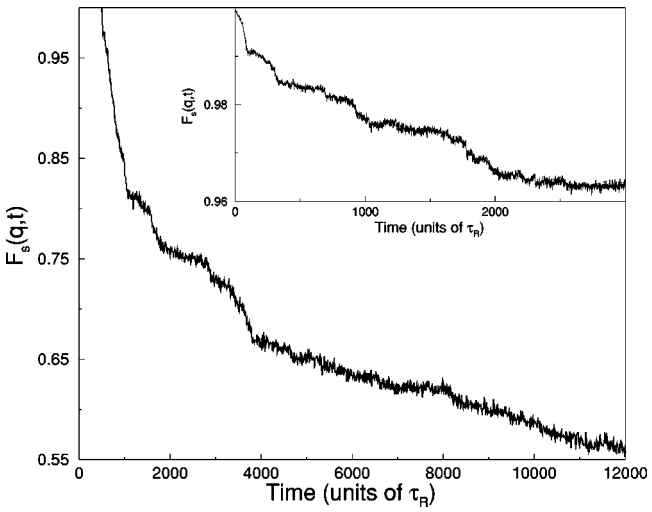

FIG. 12. Close-up of the intermediate scattering function; $qd = 6.25$, $t_w = 500\tau_R$. Inset: the same for a 500-particle system.

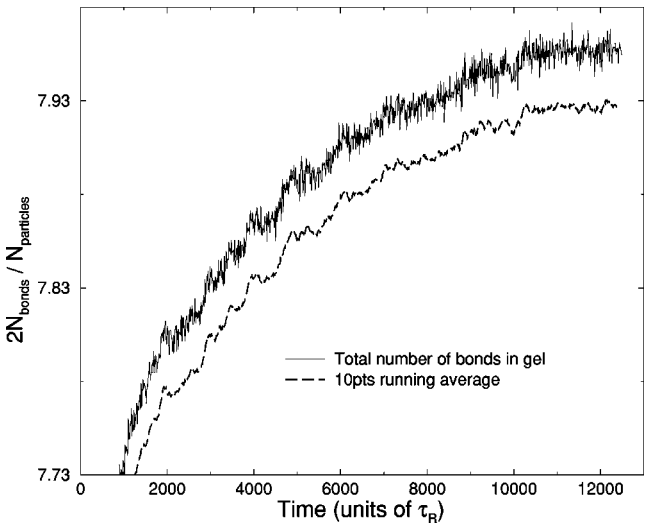

FIG. 13. Close-up of the scaled total number of bonds in the system and a ten-point running average.

yond the β relaxation, were practically unchanged, thereby showing that, whatever the relaxation mechanism, the same degree of cooperativity is present.

Now it is known that particle displacements are spatially correlated, their temporal distribution can be studied. For this we calculated the intermediate scattering function for a single gel, with no averaging procedure, i.e., over a single run. In Fig. 12 the β relaxation and the plateau are not apparent due to the linear time scale, which is useful for comparison with other microscopic results. It is apparent that the relaxation processes at work are not evenly distributed in time. A succession of plateaus and sharp drops is observed. One must remember that this function is averaged over all particles in the system; therefore a sharp drop in the averaged function must be a sign of major cooperative rearrangement. For a smaller sized system where a greater fraction of the particles is included in any given strand, the plateaus are closer to the horizontal and the fast decorrelations are sharper (see the inset of Fig. 12 for a 500-particle system).

Following on from the localization in time and in space of cooperative motion, we found similar nonuniform behavior for the total number of bonds in the system, a close-up of which is shown on Fig. 13 (scaled to show the average number of neighbors). A running average has been used to better show the underlying trends of the data. Here again fast increases are interspaced with plateaus and short time decreases. Qualitatively, we can see that both the size and gradient of the rapid increases tend to decrease as time goes on. This was also true of F_s, and the same behavior is apparent in close-ups of the energy (not shown here). It is consistent with a slowing down of relaxation processes as the gel ages.

Considering that the particles are strongly localized, it is surprising to see substantial decreases in the total number of bonds in the system. The lifetime of a bond based on a simple diffusion over a barrier argument is $\tau_{bond} \approx \tau_R e^{-U/k_B T} \approx 3100\tau_R$ for a pair of particles interacting with this potential. When taking into account the average number of neighbors within interaction range, one would not expect to find many broken bonds in any given time interval. Due to the finite range of the potential, it is possible to define bonds exactly as being within the interaction distance; therefore, we used a procedure that kept track of all particles that have had broken or created bonds within a given time interval. Remarkably, this shows that a high fraction of the particles break and create bonds during the evolution of the system. Nine percent of the particles were found to have broken bonds (slightly higher for the created bonds) when comparing configurations $500\tau_R$ apart. This is a much higher number than what would be expected from Fig. 13, which reflects only on the net number of bonds created and broken. This number is probably an underestimate since it does not include bonds broken and recreated between the same pair of particles over that time interval. Over any sizable time interval there is always a surplus of created bonds. In order to illustrate the effect of the dynamics, we show on Fig. 14 the proportion of particles that change their near neighbor envi-

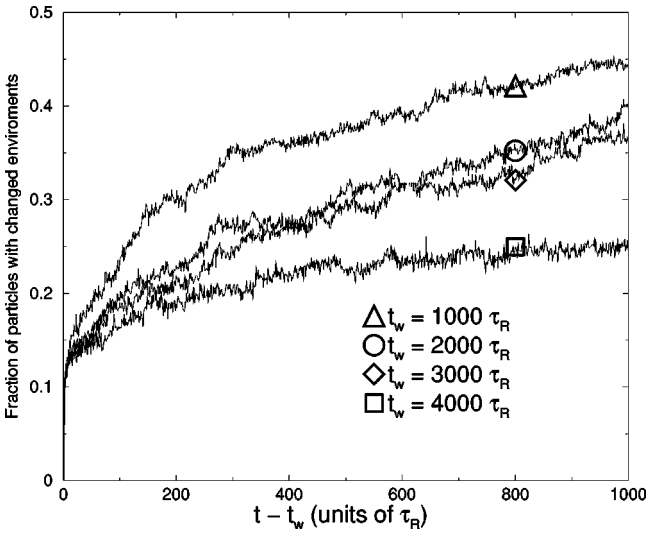

FIG. 14. Fraction of particles that change their nearest neighbor environment for increasing waiting times.

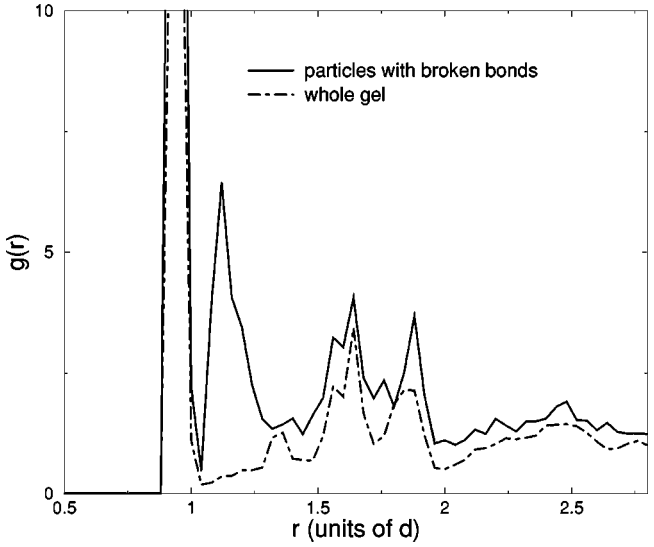

FIG. 15. Radial distribution function done with all the particles in the gel and by selecting particles with broken bonds.

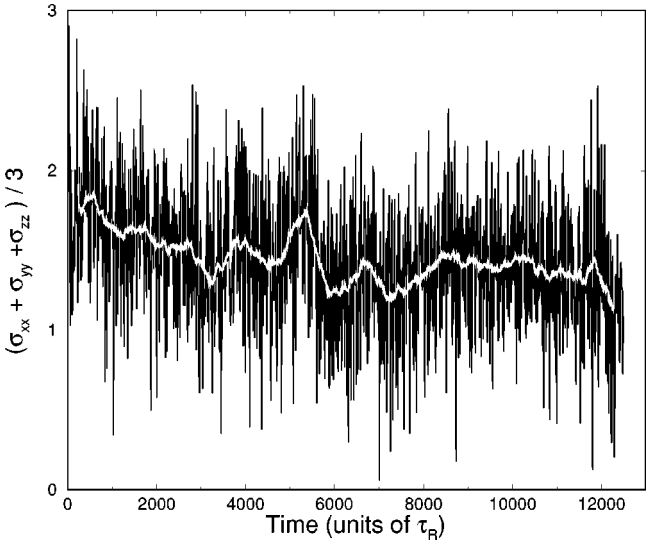

FIG. 16. Averaged normal stress tensor components (negative of pressure): raw data in black, 20-point running average in white.

ronments compared to a reference configuration chosen every $1000\tau_R$. There are three points of importance. There is a short time interval where about 5–7 % of the particles change environment within a couple of τ_R. This regime is independent of the reference configuration and corresponds to the β decay. Its age independence suggests that there is a continuous process of breaking and creating bonds at short times. This is further discussed in the next section. Figure 14 also has a second regime which is waiting time dependent and mostly follows the trends of the aging behavior, i.e., the rate at which particles change environment slows down with increasing waiting time. The third point to notice is the absolute values. For the top curve the changes in the gel involve 27 % of the particles, a huge number considering the relatively small distances moved by the particles.

The presence of particle displacements that are greater than the contribution from the elastic modes, of correlated dynamics, and of a high fraction of particles changing environments means that we expect to find some correlations in the position of those particles that have broken bonds or changed environment. However, breaking bonds in a concentrated system is always going to lead to some correlation between the particles involved; to see this, imagine pulling away one of the particles of a tetrahedron—the three particles left behind have all had a broken bond and are highly correlated in space.

A visual inspection of the gel with highlighted particles where bonds had been broken confirmed the suspected correlation; we also calculated a pair correlation function $g_b(r)$ by selecting the particles that had broken bonds in a given time interval (Fig. 15), and comparing it to the normal pair correlation $g(r)$. The correlation shows up in $g_b(r)$ as a higher first neighbor peak and a large peak beyond it that is found at the limit of the interaction potential, which is no surprise since it is by definition the distance at which one considers a bond to be broken. In terms of the previously given argument about pulling apart a tetrahedron, the higher first peak is due to the strong correlation of the particles left behind, while the second peak is due to the particles that are just beyond the interaction distance, i.e., the ones that have just broken off. This second peak at the limit of the potential is probably related to the initially rapid increase seen in Fig. 14, since it most likely shows that a lot of particles are hovering near the edge of the potential well, accounting for much of the bond breaking as they pop in and out when the strand is deformed by thermal motion.

Exactly the same observations were made about the particles that had created bonds in any reasonable time interval.

The internal stresses of the gel were also investigated. They were postulated to be the driving force of aging in other studies [20]. It is known that gels formed with periodic boundary conditions have nonzero normal stresses [45], and experimentally a gel that has been detached from the walls of its container shrinks macroscopically [20]. Figure 16 shows the average of the normal stresses, raw data in black and the running average in white. The raw data show the high frequency noise due to the Brownian fluctuations, but the presence of underlying slow fluctuations in the average value is revealed by the running average. The general trend is that of a decrease, and there are large fluctuations in the average, although not as large as any of the fluctuations in the raw data. A spatial stress correlation function $C_\sigma(R) = \langle \sigma(r)\sigma(r+R) \rangle$ was calculated, where σ is the average of the diagonal elements of the stress tensor calculated at each particle. It was found to show only very low spatial stress correlations.

The distribution of bond lengths in the gel was found to be quasiequilibrium with only a small discrepancy at distances beyond the potential minima due to the normal stresses present in the system, as can be seen on Fig. 17.

IV. DISCUSSION

This study of the dynamics of gels formed from colloids interacting via a depletion potential has showed that complex behavior arises during aging. The following discussion is

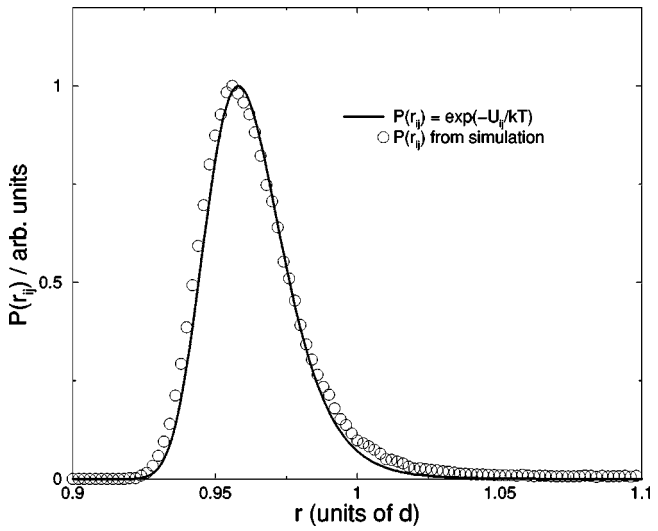

FIG. 17. Distribution of bond lengths in gel (circles). The black line is $P=\exp(-U_{ij}/kT)$. Recall that the range of the potential is $1.1d$.

structured in the same way as the presentation of the results, while trying to place the results in the context of previous findings.

A. Energy and N_{bonds}

It was found that the total potential energy of the system could be described in terms of a power law with an exponent $b=0.3$, which is a value intermediate between those obtained by Kob and Barrat for a Lennard-Jones glass ($b=0.14$) [41] and by Parisi [46] ($b=0.7$) for a Monte Carlo generated glass. However, the total number of bonds in the system was found to grow in three separate logarithmic regimes. Some of this three-regime structure was also present in the energy plot, demonstrating the difficulty in describing accurately these very slow growths and decays. The impossibility of calculating these quantities in experiments makes verification difficult if not impossible. It is, however, worth mentioning that Bouchaud's trap model [36] predicts a logarithmic dependence on time of the energy. Such logarithmic dependences can also be seen in a variety of systems, for example, crumbling thin sheets [47]. However, whether the slow growth of the number of bonds is interpreted as a power or a logarithmic law, the presence of three distinct regimes is of much interest and demonstrates the complex behavior associated with the formation and consolidation of the gel. We know from previous work that the time to percolate is less than $1\tau_R$ [14]. Following this, one would expect some fast consolidation of the network during which thin strands coarsen. Since diffusion processes occur, by definition, on the time scale of $1\tau_R$, one would expect complex and fast rearranging at relatively short times and short length scales, as was seen by Haw *et al.* for 2D colloid simulations, where compactification was obvious at short times [48]. However, given that we know that the end product of this is not at thermodynamic equilibrium, these fast rearrangement processes must be inactive at intermediate to long times (otherwise, equilibrium phases would result). Although all the regimes seen on Fig. 1 occur after percolation, it is beyond the scope of this paper to explain all three; our attention is here focused on the last one for several reasons: it is expected that the behavior may be less complex in this region; these time scales are more accessible to experiments, thereby providing interesting comparisons with the simulation results and insights that may be tested on real systems. In order to study the aging and not the formation and consolidation behavior the work showed here focuses on the behavior in the regime from $100\tau_R$ after quenching onward.

As an aside, it is worth mentioning that the noise in the energy of the gel varies as $FT(U)^2 \approx 1/f^{1.4}$, this value being closer to the $1/f$ flicker noise than the more usual $1/f^2$ white noise. This has been linked in the literature to self-organized criticality and to cooperative behavior in complex systems. However, this needs to be studied further before conclusions can be drawn from it.

B. Correlation functions: β relaxation

The self-part of the ISF calculated for this system displayed the classic two-step relaxation. Both of these relaxations were found to be well approximated by stretched exponentials with a plateau between them.

The age invariant short time dynamics corresponding to the β relaxation was interpreted in terms of the Krall-Weitz model for the decorrelation due to the elastic modes present in a gel. Although they first used it for describing low volume fraction fractal gels, the physical reality of the model is still present even though the gel is not a fractal object. This model has been shown to work well in describing gels at higher ϕ by Romer *et al.* [24] with reduced values of δ^2 and τ_c reflecting the compactness of the gels.

The mean square displacements and the β relaxation were fitted using Eqs. (11) and (12); the value of the exponent was determined to be $p=0.4\pm0.1$, which is distinctly smaller than that found by Krall and Weitz for their low ϕ polystyrene gel ($p=0.7$) [23]. Romer *et al.* also found $p=0.7$ for a high ϕ polystyrene gel [24]. However, Solomon and Varadan found $p=0.5$ for a low ϕ thermoreversible gel of silica particles [25]. In the Krall-Weitz model p is related to the length scale dependent spring constant for fractal clusters via $\kappa(s) \sim s^{-\beta}$ and $p=\beta/(\beta+1)$. From computer simulations, $\beta \sim 3.1$ for DLCA [49]; from Krall and Weitz and from Romer *et al.* $p=0.7$, $\beta=2.3$; whereas from Solomon and Varadan $p=0.5$ and therefore $\beta=1.0$ for thermoreversible gels which the authors believed had some angular rigidity on the local level due to surface roughness and a different aggregation mechanism leading to a locally denser gel. Furthermore, previous studies by one of the authors on 2D gel networks where trimers provided some angular rigidity [16] showed that for such systems $\beta \sim 1.1$–1.3. All of these results suggest, as proposed by Solomon and Varadan, that the elasticity exponent β is strongly dependent on the angular rigidity of the local network. Here $p=0.4$ and therefore $\beta=0.66$, suggesting a structure that only slowly becomes more compliant with the increasing length scale. There are several factors influencing this in these simulations. First, there is no imposed angular rigidity for the colloid interaction (this is dif-

ferent from experimental particles, which may be rough or deform under the strength of the interactions). Second, the colloid volume fraction used here is $\phi=0.3$, much higher than in most experiments. And third, the interaction range is very small $(0.1d)$; this has been shown by Lodge and Heyes [45] to affect the structures obtained when forming the gels. Long interaction distances resulted in the creation of gels where the local structure was very compact [for example it can be seen as a split second peak in $g(r)$], whereas when shorter ranged potentials were used ''fluffier'' structures resulted. Although the latter is the case in this study, at these very long times the local structure is compact as can be seen in the $g(r)$ function for the whole gel shown in Fig. 15. It is obvious that a thicker, more compact strand of colloids has a higher angular rigidity. Furthermore, this third point is strengthened by the high ϕ. This also partially negates the first point since the lack of angular rigidity of a single bond becomes irrelevant if there are no singly connected particles in the strand. This explains the high angular rigidity of this structure and hence the low values of p and β. An interesting point that arises out of this discussion is that, for a given maximum depth of potential, the rigidity of the gel may be influenced strongly by the range of the potential. This may explain why for the higher volume fraction gels of Romer *et al.* $p=0.7$, the same as for the Krall and Weitz low volume fraction gels, although the range of the interactions present in the aforementioned experimental systems was not clear.

This physical picture is confirmed by direct visualization of the gel. This shows the clusters of particles moving relative to each other on time scales of order $1\tau_R$. Furthermore, this is consistent with the high number of particles that change environment during such time intervals. This is a direct consequence of clusters in relative motion within a relatively stiff structure, thereby causing many bonds to break and reform.

The length scale dependent plateau height as characterized by f_q^s was found to have a very large q width. This result is very similar to Puertas *et al.* [30], who simulated the approach to gels in concentrated fluids near the glass transition. They obtained a similar broad dependence, showing again the strong confinement of the particles due to the short range potentials. This extends their results to a lower ϕ than they used. A further distinction is that this result is at a point on the phase diagram deep in the gel state, whereas they were in the fluid state, leading up to the gel.

C. Correlation functions: α relaxations

The α relaxation for waiting times $\geqslant 500\tau_R$ was found to be well described by a stretched exponential $F_s(q,t,t_w) = A\exp\{-[(t-t_w)/\tau_\alpha]^\mu\}$, where the exponent was always $\mu < 1.0$. This type of law is often observed and results from the presence of relaxation modes with a wide distribution of time scales. This can be written as a Laplace transform over the distribution of relaxation modes [42]: $F(t) = \int_0^\infty \rho(\gamma)e^{-\gamma t}d\gamma$. The exponent of the stretched exponential is strongly dependent on the shape of the distribution $\rho(\gamma)$, wider distributions leading to lower exponents. In this study, the variation of the exponent of the stretched exponential, $\mu=0.45\rightarrow 0.72$ as $t_w=500\tau_R\rightarrow 2250\tau_R$, clearly indicates a reduction of the width of the mode distribution. Furthermore, several observations point to the possibility of $\rho(\gamma)$ being a bimodal distribution where the short time modes are widely separated from the long time modes: the variation in μ is fast for small waiting times and levels to $\mu\sim 0.7$ for longer waiting times; there is a change in behavior for $t_w<500$ where the α relaxation appears to have a ''fast'' decay followed by a ''slow'' one, making it impossible to fit a stretched exponential. Hence the success of using a function containing two stretched exponentials to fit the decay of the α relaxation up to waiting times of $t_w=100\tau_R$. In this scheme each of the exponentials describes one part of the distribution. This behavior was reproduced by numerical integration of the Laplace transform for distributions of modes made of two widely separated Gaussians. All of the correlation function data can then be explained. μ and μ_2' describe the distribution of the ''slow'' modes, $\mu=\mu_2'=0.7\pm 0.2$ for all waiting times larger than the time for the slowest of the ''fast'' modes to relax. μ_1', which describes the distribution of the ''fast'' modes, increases toward 1.0 as the distribution of the modes that have not yet relaxed narrows. For intermediate to long waiting times, a single stretched exponential is recovered.

The q dependence of the characteristic relaxation times $\tau_\alpha, \tau_{\alpha 1}', \tau_{\alpha 2}'$ extracted from the fits also contains information about the processes at work. ν at long waiting times and $\nu_2'=2.2\pm 0.1$; for the latter exponent this was true for all the waiting times back to $t_w=100\tau_R$. This is very close to a diffusive law $\tau\sim q^{-2}$, yet with a consistent deviation. ν_1' was found to vary only very weakly with q, highlighting the fact that different mechanisms are responsible for the ''fast'' and ''slow'' relaxations. It also shows that these ''fast'' modes are not related to the Krall-Weitz elastic modes which showed up in experiments as $\tau\sim q^{-2}$.

Comparing these relaxation processes with the much better studied glasses, the α relaxation behavior is more complex in this case than for homogeneous supercooled liquids [41]. It may not be surprising that there should be some processes that would be specific to gels, considering their spatial inhomogeneity.

This framework also explains why in experiments a constant value of the stretched exponential exponent is usually found, since the ''fast'' modes observed here would be inaccessible.

D. Correlation functions: Aging

When considering the ISF in nonequilibrium systems, aging can be observed to occur as a lengthening of the plateau at intermediate times. The response becomes strongly dependent on waiting time after the quench. This was seen clearly in our data. By making the curves coincide at one point (or equivalently using the extracted parameters from the fits), a collapse within a fairly short time window was observed. It is obvious that, since the exponents of the stretched exponentials are slightly waiting time dependent, the collapse cannot be perfect over a long time scale; however, it is an important feature displayed by many gels and glasses [30]. The depen-

dence of τ_γ on the waiting time is explained from the previous deductions about our system, taking into account the fact that τ_γ is nearly equivalent to τ_α for a single stretched exponential describing the whole decay. The presence of slow and fast modes, and therefore a change of behavior once the slow modes are no longer present, was observed again in what appeared to be two different aging regimes in Fig. 8. It is in fact a confirmation of that change in behavior due to the distribution of modes going from bimodal to single peaked. Therefore, the correct value of ξ to compare to experiments is $\xi=0.66$. Previously, $\tau\sim t_w^\xi$ with $\xi=0.88$ [41] and $\xi\sim 1.1$ [44] were found for glasses, close to $\xi=1$, which would be the simple aging case.

The experimental studies of Cipelletti *et al.* reported $\nu=1$, i.e., $\tau_\alpha\sim q^{-1}$, meaning the length scale displacement scaled linearly with time. This was done for both attractive and repulsive systems, where it was thought in both cases that the relaxation of internal stresses dominate the dynamics. The theoretical argument from the same studies also explained their value of the exponent $\mu=1.5$. The aging behavior found was $\tau_\alpha\sim t_w^\xi$ with $\xi=0.9$ after a period of exponential growth for the gels [20] and $\xi=0.78$ for the repulsive system [22]. The very different values of μ and ν obtained here point to major differences in the mechanisms of aging even if the scaling of the relaxation times looks similar.

E. Real space displacements

The Van Hove correlation function gives us a more intuitive idea of the particle displacements in real space. For large observation times and long waiting times, as is the case in Fig. 10, the system is in a regime where the displacements are greater than the β plateau regime. For comparison with a system with diffusionlike displacements, a Gaussian was fitted to the peak. The very large tail present shows just how non-Gaussian the dynamics are within the α relaxation regime. The displacements around the peak and up to $0.25d$ appear to be Gaussian distributed, leaving the aforementioned large tail. Not all displacements within this tail are caused by the same physical processes. We can distinguish between two types of behavior. First, single particle movements: particles break away from the network, becoming part of the gas phase before rejoining the network somewhere else or moving along the gel by surface diffusion. These particles make up all the displacements greater than $1d$, but the numbers concerned are small (due to the high coordination of the particles in the gel), i.e., they could not account on their own for the α relaxation. Second, there are particles that have moved distances of around $0.25d<r<1d$, but which never leave the network, and for which the displacements are correlated in time and space. We also note that the part of the displacements found after the peak follows a power law with an exponent $f=2.8\pm0.4$. This is, within errors, what was deduced by Cipelletti *et al.* and predicted by Bouchaud and Pitard [50]. However, as we have just seen, their system is quite different, being strongly attractive, and other parameters such as the wave vector dependence are different from this work. Further work is necessary before conclusions can be drawn from this.

F. Cooperative dynamics

The microscopic data presented also indicate that aging does not occur as a continuous process but rather as a succession of ''events'' which occur on a time scale that increases with increasing waiting time, as was observed in a close-up of the number of bonds per particle. Indeed, it seemed that for some short time intervals the number of bonds in the system decreased. These events involve a relatively large number of particles moving cooperatively, since they can be seen even on a correlation function averaged over 4000 particles, and they dominate the gel dynamics for time scales greater than the duration of the β plateau.

While the idea of cooperative dynamics in nonequilibrium systems is not new, stringlike motion of chains of particles moving cooperatively having been observed in supercooled liquids (simulations and experiments) [51,52], the behavior seen here is more reminiscent of the work of Sanya and Sood [53], who studied a dense binary colloid mixture in which steplike displacements were observed. This was accompanied by some hopping back motion as well. It is likely that a site hopping scenario is responsible for this, whereas back and forth displacements were not observed in the gel case, although such motion may be present at shorter times.

Unsurprisingly, these correlated dynamics were linked to a correlation in the localization of the particles that have broken or created bonds for a given time interval. The relatively high number of bonds broken (and created) in the gel when comparing configurations separated by a fixed time interval is an indication of the *ease* with which thermal fluctuations of the strands disrupt the network, causing a high fraction of particles to change environment. This may be a result of the spatially inhomogeneous nature of the gel. This means that the microscopic structure of dense clusters (more or less strongly) joined together in a network will have some preferential weak points. These are usually found between the denser clusters; see West *et al.* [16] for an example in 2D of where a gel ruptures when sheared. Large thermal fluctuations are less likely to cause as much disruption in a homogeneous glassy system.

G. Stresses

Although the trend in the slowly fluctuating average value of the stress data from Fig. 16 is the result of the microscopic aging ''events'' that occur in the gel, it is now thought by the authors to be unlikely to be the driving force. While it was a surprise to find that the stresses were not spatially correlated, this may point to the fact that forces that can be sustained by the intercolloidal bonds are not very great in comparison to the stresses occasioned in the strands by the thermal fluctuations, even though they suffice to confine the individual colloid particles to the gel. Under the influence of thermal fluctuations, strands can break bonds relatively easily; this is the only explanation for the large number of bonds broken in the system. A further clue that supports this argument is the relative size of the high frequency stress fluctuations compared

to both the average value of the stress and the size of the slow fluctuations. In both cases the stresses caused by the thermal fluctuations are of much higher magnitude. This supports the idea that the internal stresses cannot be responsible for the aging, and that the slow fluctuations in the average and the generally decreasing trend of the average stress are consequences of the aging, not driving factors.

H. Aging and glasses

It is not yet clear why the relaxation times increase with waiting time; however, the mechanisms invoked here involve breaking the network under the thermal fluctuations. Presumably, the network will break preferentially at the point at which it is weakest. These weak points between the strands that make up the network would tend to disappear in time (they will keep breaking until they do). As the network becomes devoid of such weak points, we can expect the dynamics to slow down, thereby causing the aging behavior. Further work is under way to clarify this issue.

Comparison of this work with that of Kob and Barrat reveals great similarities in the overall properties of the relaxation dynamics in these gels and glasses; the same aging was seen in the correlation functions, as well as superposition of the α relaxation regime. However, it is clear from this work that the microscopic mechanisms by which the aging occurs in the gels are different from the ones observed in homogeneous glasses, the dynamics in the latter involving cooperative motion of strings of particles [51]. Similarly, comparison with the work of Puertas *et al.* [30] shows the same overall behavior, even though their simulations focused on the fluid states leading up to the gel transition. The relaxation mechanisms (although they did not report any details) were very probably similar to what was observed in [51].

The aging behavior predictions given by nonequilibrium MCT are power law regimes either side of the β plateau, a waiting dependent α relaxation time, and violation of the fluctuation-dissipation theorem. Although the predictions are not specifically tested here, our data, at least qualitatively, are not in disagreement with them. We found a stretched exponential fit to be better than a power law for the α relaxation but within a certain region near the plateau a power law is certainly possible.

The potential energy surface approach lends itself well to the interpretation of our data and to comparison with aging glasses. In this picture, the gel would be in a regime in configuration space where the system samples basins of IS's with ever decreasing energy, but with the barriers between inherent structures becoming greater than the thermal energy in the system. The slow hopping over barriers manifests itself in the gel as network rearrangements, and hence the behavior of quantities such as the total number of bonds in the system.

Based on the work of Kob *et al.* [54], who showed that an effective time dependent temperature can be defined for an aging system, Sciortino and Tartaglia [38] proposed an out of equilibrium thermodynamics framework based on the IS description of the PES. In this picture, the free energy is separated into a basin term and a configuration term, reflecting the separation of time scales in supercooled fluids. In the case of a temperature jump the system equilibrates rapidly to the bath temperature in the same basin. The exploration of configuration space takes place on a much longer time scale; hence the aging observed as the system lowers its configurational energy. This description is fitting for our system where Fig. 17 shows that the system is in quasithermal equilibrium while of course not being in thermodynamic equilibrium. For the correlation functions calculated for a Lennard-Jones binary mixture, Sciortino and Tartaglia observed stretched exponentials for the equilibrium fluid, but logarithmic decays for the out of equilibrium LJ fluid. Note that this is in fact a MCT prediction for quenches near an A_3 point. Once again, superposition of the α relaxation held and relaxation time scales increasing with t_w were found.

The different regimes seen in the evolution of the total number of bonds in the gel (Fig. 1) can then be interpreted in terms of the PES, in much the way of [38] and [54]. After the instantaneous quench the system is still fluid as aggregation begins ($0\tau_R$ to $10\tau_R$); this is followed by ridge dominated dynamics ($10\tau_R$ to $100\tau_R$), and finally the aging behavior of the last regime, dominated by the slow sampling of IS's of lower and lower energy.

The similarities of this work on supercooled fluids with ours are striking, and the only difficult point concerns the shape of the α relaxations. Whereas studies of the PES of liquids found logarithmic decays, we had two regimes of stretched exponentials. It is possible that the α relaxation is more strongly influenced by microscopic mechanisms than was previously thought. Those mechanisms could well be different due to the localization of the particles within strands rather than being distributed homogeneously; the thermal fluctuations in strands being enough to break the network, thereby causing aging, even though thermal fluctuations of a single particle are very rarely enough for them to break away from a strand.

This highlights a problem concerning general theories of the glass transition. If the microscopic details that bring about the final relaxation affect the macroscopic observations, as was seen when comparing our results with those of Cipelletti *et al.* [20] and Solomon and Varadan [25] and the aforementioned results for supercooled fluids, then a theory like MCT which works with averaged quantities is unlikely to be able to distinguish between them. On the other hand, there seems to be a greater chance to incorporate different microscopic relaxation theories when using the PES approach in order to estimate the time to explore different basins, and to understand their relation with the aging time.

V. CONCLUSIONS

To conclude this study, we can say that simulations now appear to be a reasonable way to study the short term aging of soft materials. It has allowed us to study the intermediate scattering function of an aging gel in order to compare it to experimental studies, while at the same time understanding the microscopic mechanisms responsible for aging. The con-

clusion is that for this weakly attractive, gel-forming system the aging is caused by discontinuous network rearrangements due to the thermal fluctuations. It was also possible to investigate and further strengthen the relationship between gels and glasses. A possible extension of this study would concern the possibility of reproducing experimental results for a more stress driven system to check the relationship between the α relaxation and the microscopic mechanisms.

VI. ACKNOWLEDGMENT

R.A. acknowledges the support of EPSRC and Colworth Laboratories (Unilever Research) for funding; we would also like to thank H. Lekkerkerker, W. Poon, A. Puertas, M. Fuchs, L. Starrs, L. Cipelletti, and members of the Polymers and Colloids group, especially B. Thiel and R. Blumenfeld, for many useful discussions.

[1] W. Poon, A. Pirie, and P. Pusey, Faraday Discuss. **101**, 65 (1995).
[2] S. Asakura and F. Oosawa, J. Chem. Phys. **22**, 1255 (1954).
[3] A. Vrij, Pure Appl. Chem. **48**, 471 (1976).
[4] A. Gast, W. Russell, and C. Hall, J. Colloid Interface Sci. **96**, 251 (1983).
[5] A. Gast, W. Russell, and C. Hall, J. Colloid Interface Sci. **109**, 161 (1985).
[6] H. Lekkerkerker, W. Poon, P. Pusey, A. Stroobants, and P. Warren, Europhys. Lett. **20**, 559 (1992).
[7] M. Dijkstra, J. Brader, and R. Evans, J. Phys.: Condens. Matter **11**, 10079 (1999).
[8] J. Felicity, M. Lodge, and D. M. Heyes, J. Chem. Soc., Faraday Trans. **93**, 437 (1997).
[9] J.F.M. Lodge and D.M. Heyes, J. Rheol. **43**, 219 (1999).
[10] J. Lodge and D. M. Heyes, Phys. Chem. Chem. Phys. **1**, 2119 (1999).
[11] B. Bijsterbosch, M. Bos, E. Dickinson, J. van Opheusden, and P. Walstra, Faraday Discuss. **101**, 51 (1995).
[12] E. Dickinson, J. Colloid Interface Sci. **225**, 2 (2000).
[13] M. Bos and J. van Opheusden, Phys. Rev. E **53**, 5044 (1996).
[14] K.G. Soga, J.R. Melrose, and R.C. Ball, J. Chem. Phys. **108**, 6026 (1998).
[15] K.G. Soga, J.R. Melrose, and R.C. Ball, J. Chem. Phys. **110**, 2280 (1998).
[16] A.H.L. West, J.R. Melrose, and R.C. Ball, Phys. Rev. E **49**, 4237 (1994).
[17] M. Grant and W. Russel, Phys. Rev. E **47**, 2606 (1993).
[18] H. Lekkerkerker, J. Dhont, H. Verduin, C. Smits, and J. van Duijneveldt, Physica A **213**, 18 (1995).
[19] H. Verduin and J. Dhont, J. Colloid Interface Sci. **172**, 425 (1995).
[20] L. Cipelletti, S. Manly, R.C. Ball, and D. Weitz, Phys. Rev. Lett. **84**, 2275 (2000).
[21] B. Abou, D. Bonn, and J. Meunier, Phys. Rev. E **64**, 021510 (2001).
[22] L. Ramos and L. Cipelletti, Phys. Rev. Lett. **87**, 245503 (2001).
[23] A. Krall and D. Weitz, Phys. Rev. Lett. **80**, 778 (1998).
[24] S. Romer, F. Scheffold, and P. Schurtenberger, Phys. Rev. Lett. **85**, 4980 (2000).
[25] M.J. Solomon and P. Varadan, Phys. Rev. E **63**, 051402 (2001).
[26] W. Kob, *Soft and Fragile Matter* (Institute of Physics, London, 2000).
[27] J. Bergenholtz and M. Fuchs, Phys. Rev. E **59**, 5706 (1999).
[28] J. Bergenholtz and M. Fuchs, J. Phys.: Condens. Matter **11**, 10171 (1999).
[29] J. Bergenholtz, M. Fuchs, and T. Voigtmann, J. Phys.: Condens. Matter **12**, 6575 (2000).
[30] A.M. Puertas, M. Fuchs, and M.E. Cates, Phys. Rev. Lett. **88**, 098301 (2002).
[31] P.N. Pusey and W. van Megen, Nature (London) **320**, 340 (1986).
[32] P.N. Segré, V. Prasad, A.B. Schofield, and D.A. Weitz, Phys. Rev. Lett. **86**, 6042 (2001).
[33] J.-P. Bouchaud, L. Cugliandolo, J. Kurchan, and M. Mézard, Physica A **226**, 243 (1996).
[34] L.F. Cugliandolo and J. Kurchan, Phys. Rev. Lett. **71**, 173 (1993).
[35] M. Goldstein, J. Chem. Phys. **51**, 3728 (1968).
[36] J.P. Bouchaud, J. Phys. I **2**, 1705 (1992).
[37] F.H. Stillinger, Science **267**, 1935 (1995).
[38] F. Sciortino and P. Tartaglia, J. Phys.: Condens. Matter **13**, 9127 (2001).
[39] W. Poon, L. Starrs, S. Meeker, A. Moussaïd, R. Evans, P. Pusey, and M. Robins, Faraday Discuss. **112**, 143 (1999).
[40] J. Melrose, Europhys. Lett. **19**, 51 (1992).
[41] W. Kob and J.-L. Barrat, Phys. Rev. Lett. **78**, 4581 (1997).
[42] W. Götze, *Liquids, Freezing and Glass Transition* (North-Holland, Amsterdam, 1991).
[43] H. Müssel and H. Rieger, Phys. Rev. Lett. **81**, 930 (1998).
[44] D.S. Fisher and D.A. Huse, Phys. Rev. B **38**, 386 (1988).
[45] J.F.M. Lodge and M. Heyes, J. Chem. Phys. **109**, 7567 (1998).
[46] G. Parisi, J. Phys. A **30**, L765 (1998).
[47] K. Matan, R.B. Williams, T.A. Witten, and S.R. Nagel, Phys. Rev. Lett. **88**, 076101 (2002).
[48] M. Haw, M. Sievwright, W. Poon, and P. Pusey, Adv. Colloid Interface Sci. **62**, 1 (1995).
[49] P. Meakin, I. Majid, S. Havlin, and H.E. Stanley, J. Phys. A **17**, L975 (1984).
[50] J.P. Bouchaud and E. Pitard, Eur. Phys. J. E **6**, 231 (2001).
[51] C. Donati, J.F. Douglas, W. Kob, S.J. Plimpton, P.H. Poole, and S.C. Glotzer, Phys. Rev. Lett. **80**, 2338 (1998).
[52] E.R. Weeks, J.C. Crocker, A.C. Levitt, A. Schofield, and D.A. Weitz, Science **287**, 647 (2000).
[53] S. Sanya and A.K. Sood, Phys. Rev. E **57**, 908 (1998).
[54] W. Kob, F. Sciortino, and P. Tartaglia, Europhys. Lett. **49**, 590 (2000).